Chemical Science

ROYAL SOCIETY OF CHEMISTRY

EDGE ARTICLE

View Article Online
View Journal | View Issue

Open Access Article. Published on 07 June 2024. Downloaded on 2/7/2026 11:02:57 AM.
This article is licensed under a Creative Commons Attribution-NonCommercial 3.0 Unported Licence.

Check for updates

Cite this: *Chem. Sci.*, 2024, **15**, 11402

All publication charges for this article have been paid for by the Royal Society of Chemistry

Received 21st March 2024
Accepted 4th June 2024

DOI: 10.1039/d4sc01909a

rsc.li/chemical-science

The unprecedented strong paratropic ring current of a bis-Pd^{II} complex of 5,10,23-trimesityl [28] heptaphyrin(1.1.0.0.1.0.0)†

Yang Liu, Ling Xu, Xiaorong Jin, Bangshao Yin, Yutao Rao, Mingbo Zhou, Jianxin Song * and Atsuhiro Osuka

Acid-catalyzed Friedel–Crafts-type cyclization of tetrapyrrolic BF_2 complex **1** and α,α′-dibromotripyrrin **2** gave 5,10,23-trimesityl [28]heptaphyrin(1.1.0.0.1.0.0) BF_2 complex **3BF$_2$** as a stable and moderate antiaromatic macrocycle. Demetalation of **3BF$_2$** with methanesulfonic acid followed by treatment with HCl gave free-base salt **3HCl** that holds a chloride anion at the core. This salt displays a planar structure with an inverted pyrrole and a stronger paratropic ring current. Metalation of neutral free-base **3** with $PdCl_2$ gave bis-Pd^{II} complex **3Pd$_2$** as a stable antiaromatic molecule. The ^{1}H NMR spectrum of **3Pd$_2$** displays signals due to pyrrolic β-protons in the range of −1.06 ∼ −1.90 ppm, indicating the unprecedented strong paratropic ring current.

Introduction

Stable antiaromatic molecules[1] are a promising organic structural motif because of their facile redox reactivities, three-dimensional aromaticity,[2] characteristically fast excited-state decays and small HOMO–LUMO gaps,[3] and excellent conductivities in the solid-state.[4] In the last two decades, expanded porphyrins have been demonstrated to be a nice platform to realize stable antiaromatic molecules owing to their electronically and sterically adaptable properties.[5] How to strengthen the antiaromatic character of expanded porphyrins while retaining chemical stability is an interesting issue. A paratropic ring current and a theoretical NICS value are the representative indices to evaluate the strength of antiaromaticity.

Representative examples of stable antiaromatic porphyrinoids exhibiting strong paratropic ring currents are shown in Scheme 1, which include *meso*-aryl [28]hexaphyrin(1.1.1.1.1.1) bis-Au^{III} complex **A**,[6] 5,14-dimesityl [16]tetraphyrin(1.0.1.0) Ni^{II} complex (Ni^{II} norcorrole) **B**,[7] 5,10,23-trimesityl [24]hexaphyrin(1.1.0.0.1.0) bis-Pd^{II} complex **C** [8] and 5,10,19-trimesityl [20]pentaphyrin(1.1.0.1.0) ([20]smaragdyrin) **D**.[9] Signals due to the outer β-protons are observed as a pair of doublets at 3.16 and 3.10 ppm and at 1.60 and 1.45 ppm for **A** and **B**, respectively. Correspondingly, for **C** and **D**, these signals appear in the ranges of 2.49 to 0.70 ppm and 3.88 to 2.75 ppm. The calculated NICS (nucleus-independent chemical shift) values (at the B3LYP/6-31G(d) level) within the macrocycle of **A**, **B**, **C** and **D** are largely positive (Scheme 1). Among expanded porphyrins, heptaphyrins have been poorly studied so far as compared with hexaphyrins and octaphyrins despite their interesting and characteristic reactivities and properties.[10,11] In addition, the synthetic access to heptaphyrins has been rather limited. In the

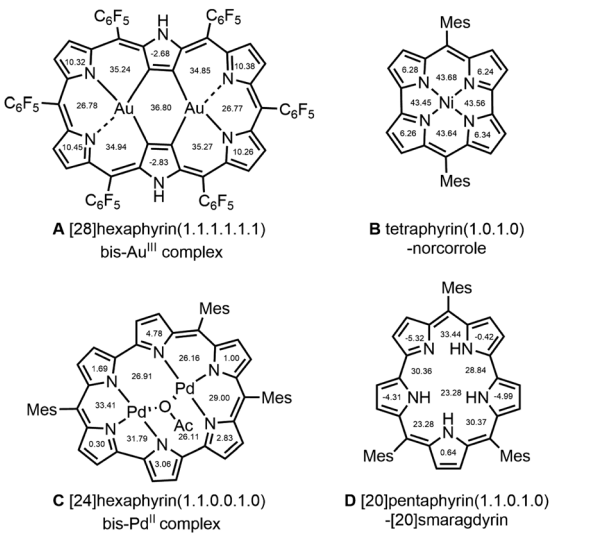

Scheme 1 Examples and NICS(0) values of stable antiaromatic expanded porphyrins, **A**, **B**, **C** and **D**; the shown NICS(0) values are determined at the geometric or areal center.

Key Laboratory of Chemical Biology and Traditional Chinese Medicine Research (Ministry of Education of China), Key Laboratory of the Assembly and Application of Organic Functional Molecules of Hunan Province, College of Chemistry and Chemical Engineering, Hunan Normal University, Changsha 410081, China. E-mail: jxsong@hunnu.edu.cn

† Electronic supplementary information (ESI) available: Details of synthetic procedures and characterization for all new compounds, NMR spectra, high resolution mass spectra, UV/vis spectra, and CV spectra. CCDC 2330167 for **3BF$_2$**, 2330168 for **3HCl** and 2330169 for **3Pd$_2$**. For ESI and crystallographic data in CIF or other electronic format see DOI: https://doi.org/10.1039/d4sc01909a

© 2024 The Author(s). Published by the Royal Society of Chemistry

Open Access Article. Published on 07 June 2024. Downloaded on 2/7/2026 11:02:57 AM. This article is licensed under a Creative Commons Attribution-NonCommercial 3.0 Unported Licence.

one-pot synthesis of *meso*-pentafluorophenyl-substituted expanded porphyrins by modified Lindsey condensation at high concentration,[12] the yield of heptaphyrin was poor (*ca.* 4–5%) and its isolation needed tedious repeated separations. Later, the same heptaphyrin was prepared in a better yield (39%) by designed acid-catalyzed condensation of tripyrrane dicarbinol and tetrapyrrane.[11b]

Results and discussion

So far, most of the expanded porphyrins have been synthesized by acid-catalyzed condensation reactions of oligopyrrolic molecules and aldehydes or their equivalents.[5] Recently, we have developed a new synthetic method for expanded porphyrins on the basis of acid-catalyzed Friedel–Crafts-type cyclization.[13] In this work, we employed a similar cyclization of tetrapyrrolic BF_2 complex **1** (ref. 14) and α,α′-dibromotripyrrin **2** (ref. 15) for the synthesis of 5,10,23-trimesityl [28]heptaphyrin(1.1.0.0.1. 0.0) **3BF$_2$**. Namely, a solution of equimolar amounts of **1** and **2** in CH_2Cl_2 was heated in the presence of *p*-toluenesulfonic acid at 50 °C for 8 h. After the usual work up, separation through an Al_2O_3 column gave **3BF$_2$** in 23% yield. The parent ion peak of **3BF$_2$** was observed at m/z = 893.4298, calcd for $(C_{58}H_{50}BF_2N_7)^+$ = 893.4233 ($[M]^+$) by high resolution MALDI-TOF mass spectrometry.

The structure of **3BF$_2$** has been revealed by X-ray analysis.[16] Two different structures (**3BF$_2$A** and **3BF$_2$B**) were found in the crystal (Fig. 1a–d). The two structures are similar, showing that the tetrapyrrolic and the tripyrrolic parts are planar but these two units are bent with an angle of *ca.* 50°. On the basis of Cα–N–Cα′ angles of the pyrroles, the pyrroles C, E, and G have been denoted as an aminic pyrrole and the pyrroles D and F have been denoted as an iminic pyrrole. The ^{1}H NMR spectrum of **3BF$_2$** in $CDCl_3$ shows three pairs of doublets in the range of 5.42–4.98 ppm and a singlet at 4.79 ppm due to the pyrrolic β-protons, indicating a moderate paratropic ring current arising from its 28π-electronic circuit. Signals due to the inner NH protons are not observed at room temperature in $CDCl_3$ but are observed at 18.18 ppm (2H) and at 17.73 ppm (1H) at 213 K, in line with the assigned structure. This phenomenon is common in expanded porphyrins, possibly due to rapid NH proton exchange between neighboring amino and imine pyrroles, or between amino pyrroles and solvent molecules like water. The absorption spectrum of **3BF$_2$** shows two prominent bands at 464 and 524 nm along with a broad tail at 1200 nm, which are typical of antiaromatic porphyrinoids (Fig. 4).[17]

In the next step, a solution of **3BF$_2$** in CH_2Cl_2 was refluxed in the presence of methanesulfonic acid overnight. After the usual work up, the organic extract was treated with an aqueous $NaHCO_3$ solution and then brine. From this residue, **3HCl** was obtained in 87% yield as red solids (Scheme 2). The parent ion peak was observed at m/z = 846.4279, calcd for $(C_{58}H_{52}N_7)^+$ = 846.4279 ($[M–Cl]^+$). The structure of **3HCl** has been revealed by X-ray analysis to be roughly C_{2v} symmetric and considerably planar with a mean-plane-deviation (MPD) of 0.358 Å (Fig. 2).[16] On the basis of the Cα–N–Cα angles (Fig. S25†), the pyrroles **A**, **C**, **D**, **E**, and **F** have been denoted as aminic and the pyrroles **B** and **G** have been denoted as iminic. Interestingly, pyrrole **A** is inverted and the Cl anion is held by hydrogen bonding interaction with the four pyrrolic NH bonds possibly, as well as the two β-pyrrolic CH protons. Similar anion binding has been

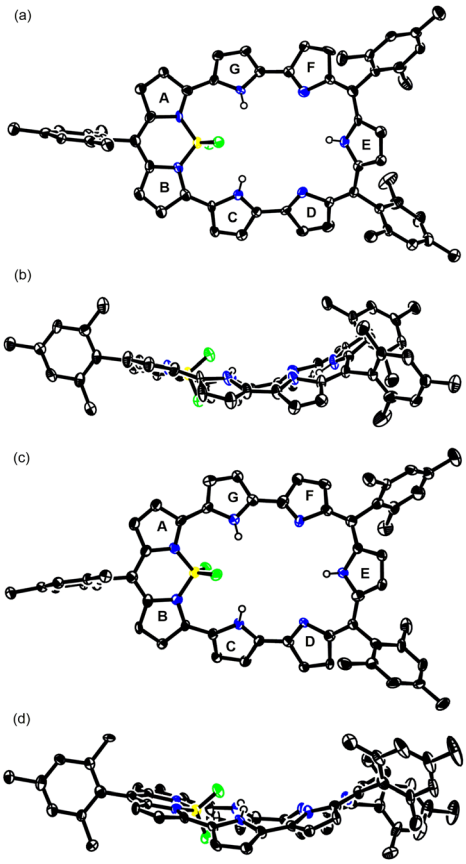

Fig. 1 Single-crystal X-ray structures of the (a) top view and (b) side view of 3BF$_2$A, and (c) top view and (d) side view of 3BF$_2$B. The thermal ellipsoids are at 50% probability.

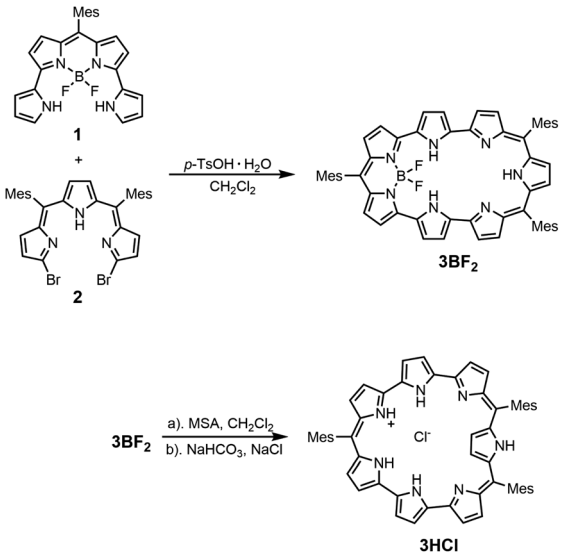

Scheme 2 Synthesis of 3BF$_2$ and 3HCl.

Open Access Article. Published on 07 June 2024. Downloaded on 2/7/2026 11:02:57 AM.
This article is licensed under a Creative Commons Attribution-NonCommercial 3.0 Unported Licence.

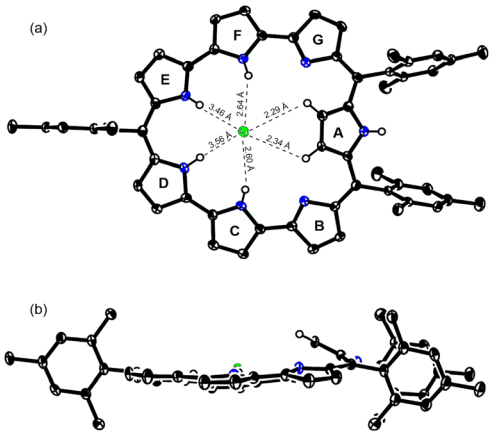

Fig. 2 Single-crystal X-ray structures of the (a) top view and (b) side view of **3HCl**. The thermal ellipsoids are at 50% probability.

extensively studied by Sessler *et al.*, but the involvement of β-pyrrolic CH protons is rare.[18] The ^{1}H NMR spectrum of **3HCl** shows signals at 25.42 and 24.89 ppm due to the inner NH protons, a signal at 4.76 ppm due to the outer NH proton, a signal at 16.79 ppm due to the inner pyrrolic β-proton, and twelve signals in the range of 4.47–3.55 ppm due to the outer pyrrolic β-protons, indicating a stronger paratropic ring current in the nonsymmetric structure. It is considered that **3HCl** takes a nonsymmetric tautomeric structure in $CDCl_3$ solution. The absorption spectrum of **3HCl** shows a split strong band at 396 and 491 nm with a shoulder at ~617 nm and a very weak and broad tail at 1600 nm (Fig. 4).

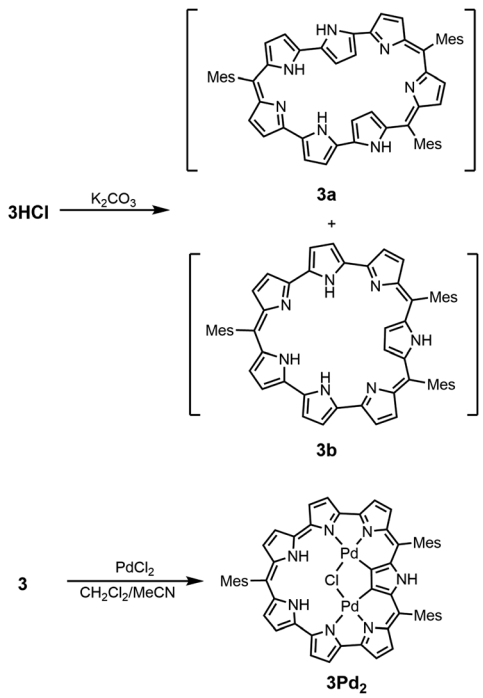

Scheme 3 Synthesis of **3** (major isomer **3a** and minor isomer **3b**) and $3Pd_2$.

Treatment of **3HCl** with a K_2CO_3 solution gave free base heptaphyrin **3** (Scheme 3). The ^{1}H NMR spectrum of **3** in DMSO-d_6 shows two isomers in a ratio of *ca.* 2 : 1. These isomers were not separable. The major isomer is non-symmetric, displaying four peaks due to the pyrrolic β-protons at 9.95, 10.11, 10.76 and 10.97 ppm, indicating the presence of two inverted pyrroles. Signals due to the outer pyrrolic β-protons of the major isomer are in range of 5.02–6.08 ppm with two inner NH protons at 19.08 and 19.25 ppm. The minor isomer is symmetric with one inverted pyrrole on the symmetry axis, showing six peaks due to outer pyrrolic β-protons in the range of 5.9–4.9 ppm, one inner pyrrolic β-proton at 10.96 ppm, two peaks due to inner NH protons at 17.43 (1H) and 15.46 (2H) ppm and one peak due to an outside NH proton at 7.05 ppm. The solubility of **3** in $CDCl_3$ is poor and the ^{1}H NMR spectrum of **3** in $CDCl_3$ is also complicated, showing four doublets due to the pyrrolic β-protons in the range of 11.2–9.5 ppm, suggesting the presence of a minor isomer having two inverted pyrroles. Signals due to the outer pyrrolic β-protons of major and minor isomers are observed in the range of 5.2–6.2 ppm.

Finally, the reaction of **3** with $PdCl_2$ in a mixture of CH_2Cl_2 and acetonitrile at room temperature for 4 h gave bis-Pd complex $\mathbf{3Pd_2}$ in 19% yield (Scheme 3). The parent ion peak was observed at $m/z = 1091.1711$, calcd for $(C_{58}H_{48}ClN_7Pd_2)^+ = 1091.1745$ ($[M + H]^+$). The structure of $\mathbf{3Pd_2}$ has been revealed by X-ray analysis to be C_{2v} symmetric and very planar with a small MPD of 0.05 Å (Fig. 3).[16] Similarly to **3HCl**, only pyrrole **A** is inverted and the remaining pyrroles are pointing inward. The two Pd metals are bound to the two pyrrolic nitrogen atoms (the pyrroles **B** and **G** and the pyrroles **C** and **F**), the β-proton of the pyrrole **A**, and the Cl^- anion with bond lengths of 1.979 Å, 2.192 Å, 1.958 Å, and 2.323 Å, respectively. The Cl^- anion is shared by the two Pd metals and interact with the NH protons of the pyrroles **D** and **E** by hydrogen bonding. In the ^{1}H NMR spectrum of $\mathbf{3Pd_2}$, a signal due to the inner NH protons is observed at a very low field (42.93 ppm), signals due to the outer pyrrolic β-protons are observed at a high field (−1.06 ~ −1.90 ppm), and a signal due to the outer NH proton is observed at −6.17 ppm,

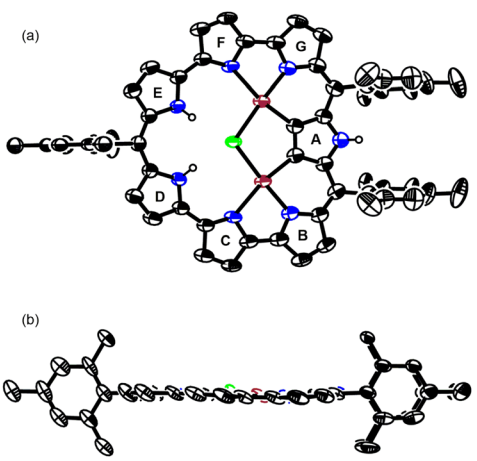

Fig. 3 Single-crystal X-ray structures of the (a) top view and (b) side view of $3Pd_2$. The thermal ellipsoids are at 50% probability.

© 2024 The Author(s). Published by the Royal Society of Chemistry

Open Access Article. Published on 07 June 2024. Downloaded on 2/7/2026 11:02:57 AM.
This article is licensed under a Creative Commons Attribution-NonCommercial 3.0 Unported Licence.

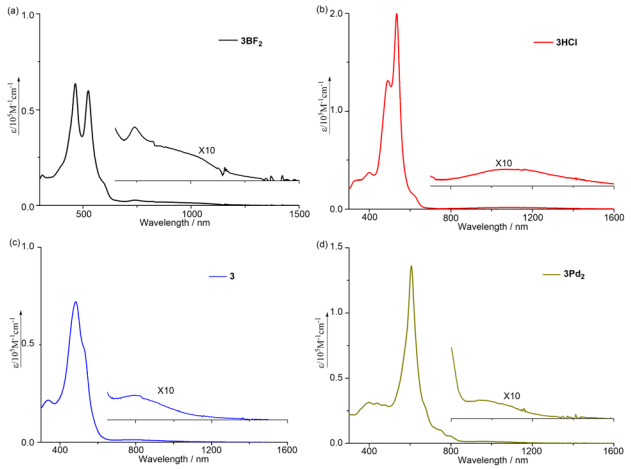

Fig. 4 Absorption spectra of $3BF_2$ (black solid line), **3HCl** (red solid line), **3** (blue solid line) and $3Pd_2$ (brown solid line) in CH_2Cl_2. For clarity, the absorbances at long wavelength are amplified by 10 times.

indicating a very strong paratropic ring current. While many antiaromatic porphyrinoids have been reported so far, the observation of pyrrolic β-protons at negative chemical shifts is unprecedented. The absorption spectrum of $3Pd_2$ shows a band at 606 nm with a weak and broad tail at 1200 nm (Fig. 4).

The electrochemical properties were investigated by cyclic voltammetry and differential pulse voltammetry (Table 1). The electrochemical HOM–LUMO gaps of $3BF_2$ and **3** are certainly small (1.25 eV and 1.30 eV), but those of **3HCl** and $3Pd_2$ are distinctly smaller, being 0.74 and 0.72 eV, respectively.

To evaluate the antiaromaticity of $3BF_2$, **3HCl**, and $3Pd_2$, NICS values and ICSS (iso-chemical shielding surface)[19] were calculated. These results are displayed in Fig. S49–S53 (ESI†).[20] The NICS values calculated in the inner area of $3BF_2$ fall within the range of 9–15 ppm, suggesting its relatively weak antiaromatic character. In contrast, the NICS values for **3HCl** were found to be in the range of 15–24 ppm, indicating enhanced antiaromaticity, potentially attributed to its more planar structure compared to $3BF_2$. Notably, for $3Pd_2$, the corresponding NICS values are significantly larger, ranging from 30 to 65 ppm, consistent with the observed strong paratropic ring current. As shown in Fig. 5, the deshielding isosurface ranges indicated by blue increase in the order of $3BF_2$ < **3HCl** < $3Pd_2$ (Fig. 4a–f). Additionally, the $ICSS_{ZZ}(1)$ plot for $3Pd_2$ was calculated to reach near −100 ppm in the inner area,[21] indicating that $3Pd_2$ is strongly antiaromatic. It is conceivable that strong paratropic ring current is stemming from the planar, rigid, large and symmetric electronic π-network of $3Pd_2$.

The benchmark for aromaticity is often determined by the maximum difference in chemical shifts ($\Delta\delta$) between the peripheral CH or NH moieties and the interior CH or NH moieties. Similarly, we can also use $\Delta\delta$ to evaluate the strength of paratropic ring current. For $3BF_2$, the value of $\Delta\delta_{CH-NH}$ is 13.43 ppm. For **3HCl**, the values of $\Delta\delta_{CH-NH}$, $\Delta\delta_{NH-NH}$ and $\Delta\delta_{CH-CH}$ are 21.87 ppm, 20.66 ppm and 13.24 ppm, respectively. For **3a** (major isomer of **3**), the value of $\Delta\delta_{CH-NH}$ is 14.23 ppm while the values of $\Delta\delta_{CH-NH}$ and $\Delta\delta_{NH-NH}$ are 12.48 ppm and 10.38 ppm for **3b** (minor isomer of **3**). For $3Pd_2$, the values of $\Delta\delta_{CH-NH}$ and $\Delta\delta_{NH-NH}$ are 43.83 ppm and 49.10 ppm. This huge $\Delta\delta$ has never been seen in other porphyrinoids, which demonstrates the unprecedented strong paratropic ring current of $3Pd_2$.

To get further insights into the origin of the strong paratropic ring current of $3Pd_2$, we also calculated the NICS values of related structures with only atoms changing or replacement based on the optimized geometry structure of $3Pd_2$ (Fig. S54 and S57†). The results show that the effects of the replacement of Cl by Br, I or OH on the paratropic ring current of $3Pd_2$ are negligible and replacement of the *meso*-Mes group with hydrogen, the NICS values at those points become even larger, suggesting that the Mes group may have a negative impact on the strength of its paratropic ring current. However, upon removal of the coordinated Pd_2Cl group, the paratropic ring current is noticeably weakened, as indicated by a decrease in NICS values from *ca.* 60 ppm to *ca.* 40 ppm at specific points within the macrocycle. Additionally, substituting Pd^{II} with Ni^{II} or Cu^{II} demonstrates that both Ni^{II} and Cu^{II} complexes exhibit strong paratropic ring currents, which are comparable to those observed in $3Pd_2$. These findings suggest that other transition metal cations may produce a similar effect, provided the complex's geometry remains essentially unaltered (Fig. S55 and S56†). Therefore, the coordination of the metal to the porphyrinoid may increase the electron density on the macrocycle, possibly due to backbonding interactions, thereby enhancing the paratropic ring current in antiaromatic porphyrinoids.

As a complement to the study of the chemical properties of heptaphyrin(1.1.0.0.1.0.0), we also investigated the reduction reaction of $3BF_2$ and the oxidation reaction of $3Pd_2$. Treating $3BF_2$ with $NaBH_4$ does not produce any reducing product while $3BF_2$ can be reduced with $Me_{10}Fc$ in the presence of a large amount of HCl, similar to the case of the annulated rosarin/octaphyrin reported by Sessler and coworkers.[22,23] The reduction product may be aromatic as judged by the absorption spectrum (Fig. S59†) but

Table 1 Electrochemical properties of $3BF_2$, **3HCl**, and $3Pd_2$ [a]

Sample	$E_{red.3}$ (V)	$E_{red.2}$ (V)	$E_{red.1}$ (V)	$E_{ox.1}$ (V)	$E_{ox.2}$ (V)	$E_{ox.3}$ (V)	ΔE_{HL} [b]
$3BF_2$	—	−1.37	−1.15	0.10	0.42	—	1.25
3HCl	−1.57	−1.23	−0.78	−0.04	0.39	—	0.74
3	−1.76	−1.45	−1.16	−0.14	0.15	0.34	1.30
$3Pd_2$	−1.79	−1.33	−0.95	−0.23	0.25	—	0.72

[a] Measured in anhydrous CH_2Cl_2 with 0.1 M nBu_4NPF_6 in a glovebox *versus* ferrocene/ferrocenium ion couple; working electrode, glassy carbon; counter electrode, Pt wire; reference electrode, Ag/0.01 M $AgNO_3$. [b] $\Delta E_{HL} = e(E_{ox.1} - E_{red.1})$ [eV].

Open Access Article. Published on 07 June 2024. Downloaded on 2/7/2026 11:02:57 AM. This article is licensed under a Creative Commons Attribution-NonCommercial 3.0 Unported Licence.

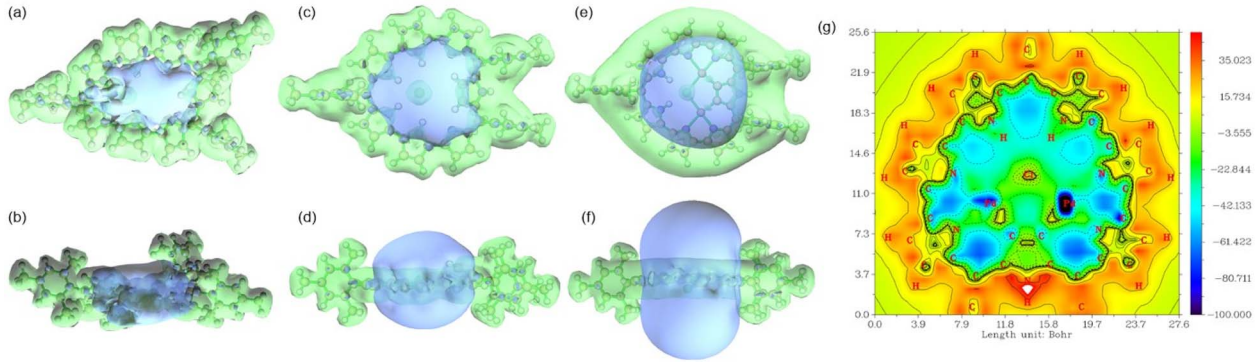

Fig. 5 ICSS of $3BF_2$, (a) top view and (b) side view; **3HCl**, (c) top view and (d) side view; $3Pd_2$, (e) top view and (f) side view. The green isosurfaces represent the region of magnetic shielding values larger than 5.0 ppm. The blue isosurfaces represent the region of magnetic deshielding values smaller than −5 ppm. (g) $ICSS_{ZZ}(1)$ plot of $3Pd_2$.

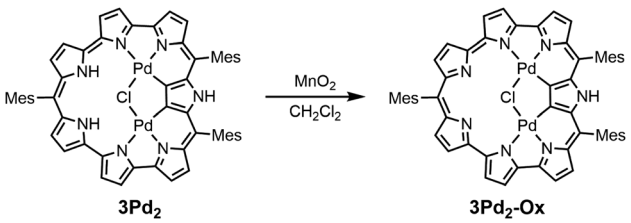

Scheme 4 Synthesis of $3Pd_2$-Ox.

is too unstable to be isolated from the reaction mixture. The oxidation of $3Pd_2$ with MnO_2 produces an aromatic counterpart $3Pd_2$-Ox in 52% yield (Scheme 4), and it is spontaneously reduced in solvent (Fig. S62†). The parent ion peak of $3Pd_2$-Ox can be observed at m/z = 1088.1606, calcd for $(C_{58}H_{46}ClN_7Pd_2)^+$ = 1088.1668 ($[M + H]^+$). The ^1H NMR spectrum of $3Pd_2$-Ox in $CDCl_3$ shows four sharp peaks and two broad peaks in the range of 11.25–9.64 ppm due to the pyrrolic β-protons, indicating a clear diatropic ring current arising from its 26π-electronic circuit. Broad peaks at 11.10 ppm and 9.94 ppm can be due to the β-protons and those in the range of −2.5 to −3.5 ppm may be ascribed to a tautomer of $3Pd_2$-Ox (Fig. S61†).

Conclusions

In summary, [28]heptaphyrin(1.1.0.0.1.0.0) BF_2 complex $3BF_2$ was synthesized by acid-catalyzed Friedel–Crafts-type cyclization of tetrapyrrolic BF_2 complex **1** with α,α′-dibromotripyrrin **2**, and was converted to its HCl salt **3HCl** and bis-Pd complex $3Pd_2$. While these heptaphyrins are all antiaromatic, $3Pd_2$ displays an unprecedentedly strong paratropic ring current. Additionally, we conducted research on the reduction of $3BF_2$ and the oxidation of $3Pd_2$. The unprecedentedly strong paratropic ring current can be attributed to its planar, rigid, large, and symmetric π-network, as well as possible backbonding interactions that augment the electron density on the macrocycle brought about by Pd^{II} coordination. Along this direction, new synthetic trials to explore even stronger antiaromatic molecules are in progress in our laboratory.

Data availability

All experimental data and detailed experimental procedures are available in the ESI.†

Author contributions

J. Song conducted the project. Y. Liu performed most of the synthesis and characterization, and partial DFT calculations. L. Xu carried out partial crystal analysis and partial DFT calculations. X. Jin contributed to partial synthesis. B. Yin conducted partial NMR tests. Y. Rao and M. Zhou assisted with partial crystal analysis. Y. Liu, L. Xu, Y. Rao, J. Song and A. Osuka prepared the manuscript.

Conflicts of interest

There are no conflicts to declare.

Acknowledgements

The work was supported by the National Natural Science Foundation of China (Grant No. 22071052, 21772036, 22271091, and 22201072), Science and Technology Planning Project of Hunan Province (2018TP1017), and Science and Technology Innovation Program of Hunan Province (2021RC4059).

Notes and references

1 (*a*) R. Breslow, *Acc. Chem. Res.*, 1973, **6**, 393; (*b*) H. Hopf, *Angew. Chem., Int. Ed.*, 2013, **52**, 12224; (*c*) S. Nobuse, H. Miyoshi, A. Shimizu, I. Hisaki, K. Fukda, M. Nakano and Y. Tobe, *Angew. Chem., Int. Ed.*, 2015, **54**, 2090.

2 (*a*) R. Nozawa, H. Tanaka, W.-Y. Cha, Y. Hong, I. Hisaki, S. Shimizu, J.-Y. Shin, T. Kowalczyk, S. Irle, D. Kim and H. Shinokubo, *Nat. Commun.*, 2016, **7**, 13620; (*b*) R. Nozawa, J. Kim, J. Oh, A. Lamping, Y. Wang, S. Shimizu, I. Hisaki, T. Kowalczyk, H. Fliegl, D. Kim and H. Shinokubo, *Nat. Commun.*, 2019, **10**, 3576.

© 2024 The Author(s). Published by the Royal Society of Chemistry

Open Access Article. Published on 07 June 2024. Downloaded on 2/7/2026 11:02:57 AM. This article is licensed under a Creative Commons Attribution-NonCommercial 3.0 Unported Licence.

3 J.-Y. Shin, K. S. Kim, M.-C. Yoon, J. M. Kim, Z. S. Yoon, A. Osuka and D. Kim, *Chem. Soc. Rev.*, 2010, **39**, 2733.
4 J. Liu, J. Ma, K. Zhang, P. Ravat, P. Machata, S. Avdoshenko, F. Hennersdorf, H. Komber, W. Pisula, J. J. Weigand, A. A. Popov, R. Beerger, K. Müllen and X. Feng, *J. Am. Chem. Soc.*, 2017, **139**, 7513.
5 (*a*) J. L. Sessler and D. Seidel, *Angew. Chem., Int. Ed.*, 2003, **42**, 5134; (*b*) S. Saito and A. Osuka, *Angew. Chem., Int. Ed.*, 2011, **50**, 4342; (*c*) M. Stepien, N. Sprutta and L. Latos-Grażyński, *Angew. Chem., Int. Ed.*, 2011, **50**, 4288; (*d*) T. Tanaka and A. Osuka, *Chem. Rev.*, 2017, **117**, 2584; (*e*) B. Szyszko, M. J. Bialek, E. Pacholska-Dudziak and L. Latos-Grażyński, *Chem. Rev.*, 2017, **117**, 2839; (*f*) M. Stępień, E. Gońka, M. Żyła and N. Sprutta, *Chem. Rev.*, 2017, **117**, 3479; (*g*) A. Borissov, Y. Kumar Maurya, L. Moshniaha, W.-S. Wong, M. Żyła-Karwowska and M. Stępień, *Chem. Rev.*, 2022, **122**, 565.
6 S. Mori and A. Osuka, *J. Am. Chem. Soc.*, 2005, **127**, 8030.
7 T. Ito, Y. Hayashi, S. Shimizu, J.-Y. Shin, N. Kobayashi and H. Shinokubo, *Angew. Chem., Int. Ed.*, 2012, **51**, 8542.
8 Y. Liu, L. Xu, Y. Rao, B. Yin, M. Zhou, J. Song and A. Osuka, *Org. Lett.*, 2023, **25**, 8121.
9 D. X. Y. Liu, Y. Rao, G. Kim, M. Zhou, D. Yu, L. Xu, B. Yin, S. Liu, T. Tanaka, N. Aratani, A. Osuka, Q. Liu, D. Kim and J. Song, *J. Am. Chem. Soc.*, 2018, **140**, 16553.
10 (*a*) S. Hiroto, H. Shinokubo and A. Osuka, *J. Am. Chem. Soc.*, 2006, **128**, 6568; (*b*) S. Saito and A. Osuka, *Chem.—Eur. J.*, 2006, **12**, 9095; (*c*) S. Saito, K. S. Kim, Z. S. Yoon, D. Kim and A. Osuka, *Angew. Chem., Int. Ed.*, 2007, **46**, 5591; (*d*) S. Saito, J.-Y. Shin, J. M. Lim, K. S. Kim, D. Kim and A. Osuka, *Angew. Chem., Int. Ed.*, 2008, **47**, 9657; (*e*) S. Saito, K. Furukawa and A. Osuka, *Angew. Chem., Int. Ed.*, 2009, **48**, 8086; (*f*) R. Sakamoto, S. Saito, S. Shimizu, Y. Inokuma, N. Aratani and A. Osuka, *Chem. Lett.*, 2010, **39**, 439; (*g*) T. Yoneda, S. Saito, H. Yorimitsu and A. Osuka, *Angew. Chem., Int. Ed.*, 2011, **50**, 3475; (*h*) M.-C. Yoon, J.-Y. Shin, J. M. Lim, S. Saito, T. Yoneda, A. Osuka and D. Kim, *Chem.—Eur. J.*, 2011, **17**, 6707; (*i*) T. Higashino, B. S. Lee, J. M. Lim, D. Kim and A. Osuka, *Angew. Chem., Int. Ed.*, 2012, **51**, 13105; (*j*) W.-Y. Cha, T. Yoneda, S. Lee, J. Mi. Lim, A. Osuka and D. Kim, *Chem. Commun.*, 2014, **50**, 548; (*k*) J. O. Kim, Y. Hong, T. Kim, W.-Y. Cha, T. Yoneda, T. Soya, A. Osuka and D. Kim, *J. Phys. Chem. Lett.*, 2018, **9**, 4527.
11 (*a*) J. L. Sessler, D. Seidel and V. Lynch, *J. Am. Chem. Soc.*, 1999, **121**, 11257; (*b*) G. Anguera, B. Kauffmann, J. L. Borrell, S. Borros and D. Sanchez-Garcia, *Org. Lett.*, 2015, **17**, 2194; (*c*) T. Kohler, D. Seidel, J. L. Sessler, Z. Ou, K. M. Kadish and J. L. Sessler, *J. Am. Chem. Soc.*, 2003, **125**, 6872; (*d*) V. R. G. Anand, S. K. Pushpan, A. Srinivasan, S. J. Narayanan, B. Srideri and T. K. Chandrashekar, *Org. Lett.*, 2000, **2**, 3829; (*e*) V. G. Anand, S. K. Pushpan, S. Venkaratraman, A. Dey, T. K. Chadrashekar, R. Roy, B. S. Joshi, S. Deepa and G. N. Sastry, *J. Org. Chem.*, 2002, **67**, 6309; (*f*) C. Bucher, D. Seidel, V. Lynch and J. L. Sessler, *Chem. Commun.*, 2002, 328.
12 J.-Y. Shin, H. Furuta, K. Yoza, S. Igarashi and A. Osuka, *J. Am. Chem. Soc.*, 2001, **123**, 7190.
13 W. Deng, Y. Liu, D. Shimizu, T. Tanaka, A. Nakai, Y. Rao, L. Xu, M. Zhou, A. Osuka and J. Song, *Chem.—Eur. J.*, 2023, **29**, e202203484.
14 T. Jiang, P. Zhang, C. Yu, J. Yin, L. Jiao, E. Dai, J. Wang, Y. Wei, X. Mu and E. Hao, *Org. Lett.*, 2014, **16**, 1952.
15 M. Umetani, J. Kim, T. Tanaka, D. Kim and A. Osuka, *Chem. Commun.*, 2019, **55**, 10547.
16 Deposition numbers 2330167 for **3BF$_2$**, 2330168 for **3HCl**, and 2330169 and for **3Pd$_2$** contain the supplementary crystallographic data for this paper.†
17 J.-Y. Shin, K. S. Kim, M.-C. Yoon, J. M. Kim, Z. S. Yoon, A. Osuka and D. Kim, *Chem. Soc. Rev.*, 2010, **39**, 2751.
18 J. L. Sessler, M. Cyr, H. Furuta, V. Kral, T. Mody, T. Morishima, M. Shionoya and S. Weghorn, *Pure Appl. Chem.*, 1993, **65**, 393.
19 S. Kloda and E. Kleinpeter, *J. Chem. Soc., Perkin Trans. 2*, 2001, 1893.
20 T. Lu and F.-W. Chen, *J. Comput. Chem.*, 2012, **33**, 580.
21 Z. Liu, T. Lu and Q. Chen, *Carbon*, 2020, **165**, 468.
22 M. Ishida, S.-J. Kim, C. Preihs, K. Ohkubo, J. M. Lim, B. S. Lee, J. S. Park, V. M. Lynch, V. V. Roznyatovskiy, T. Sarma, P. K Panda, C.-H. Lee, S. Fukuzumi, D. Kim and J. L. Sessler, *Nat. Chem.*, 2013, **5**, 15.
23 T. Sarma, G. Kim, S. Sen, W.-Y. Cha, Z. Duan, M. D. Moore, V. M. Lynch, Z. Zhang, D. Kim and J. L. Sessler, *J. Am. Chem. Soc.*, 2018, **140**(38), 12111.

© 2024 The Author(s). Published by the Royal Society of Chemistry